A Minimal Peptide Scaffold for β-Turn Display: Optimizing a Strand Position in Disulfide-Cyclized β-Hairpins

Andrea G. Cochran,*,† Ricky T. Tong,† Melissa A. Starovasnik,† Eleanor J. Park,† Robert S. McDowell,†,‡ J. E. Theaker,§ and Nicholas J. Skelton†

Contribution from the Departments of Protein Engineering and Bioorganic Chemistry, Genentech, Inc., 1 DNA Way, South San Francisco, California 94080

Received September 13, 2000

Abstract: Phage display of peptide libraries has become a powerful tool for the evolution of novel ligands that bind virtually any protein target. However, the rules governing conformational preferences in natural peptides are poorly understood, and consequently, structure−activity relationships in these molecules can be difficult to define. In an effort to simplify this process, we have investigated the structural stability of 10-residue, disulfide-constrained β-hairpins and assessed their suitability as scaffolds for β-turn display. Using disulfide formation as a probe, relative free energies of folding were measured for 19 peptides that differ at a one strand position. A tryptophan substitution promotes folding to a remarkable degree. NMR analysis confirms that the measured energies correlate well with the degree of β-hairpin structure in the disulfide-cyclized peptides. Reexamination of a subset of the strand substitutions in peptides with different turn sequences reveals linear free energy relationships, indicating that turns and strand−strand interactions make independent, additive contributions to hairpin stability. Significantly, the tryptophan strand substitution is highly stabilizing with all turns tested, and peptides that display model turns or the less stable C′−C″ turn of CD4 on this tryptophan "stem" are highly structured β-hairpins in water. Thus, we have developed a small, structured β-turn scaffold, containing only natural L-amino acids, that may be used to display peptide libraries of limited conformational diversity on phage.

Introduction

The surface loops of proteins and bioactive peptides have often been implicated in recognition by protein binding partners. Accordingly, it is of interest to investigate these loops as potential leads for drug discovery. Most small peptides are highly flexible and do not, therefore, adopt unique solution conformations; in particular, they do not adopt the structure that the same sequence adopts in a native protein. The lack of fixed structure reduces the affinity the peptide might have for a target (for entropic reasons) and obscures any connection between its solution properties and the active, bound-state conformation. Because of this, many strategies have been developed to introduce constraints into peptides (disulfides or other cross-links, D-amino acids, and backbone modifications)[1] or to display key functional groups on more rigid, non-peptide scaffolds.[2] Indeed, such peptidomimetics have been widely used to test structure−activity relationships, and they have been used as frameworks for synthetic combinatorial libraries.[3]

A complementary strategy for peptide-based lead discovery is display of libraries on filamentous bacteriophage.[4,5] This method allows the preparation of libraries as large as 10^{10}−10^{12} members,[4] many orders of magnitude larger than libraries that may be prepared synthetically. Furthermore, rapid and inexpensive selection protocols are available for identifying those library members that bind to a target of interest. However, only natural peptides composed of L-amino acids may be displayed on phage, so the problem of defining three-dimensional structure−activity relationships is more difficult than it might be for a constrained peptidomimetic. One possible solution to this problem is to use the structural constraints of a folded protein to present small variable peptide segments. Indeed, several small, stable proteins have been proposed as peptide display scaffolds.[6−8] Unfortunately, it is not clear that protein ligands obtained by this approach could be transformed to small-molecule drug leads. Epitope transfer from proteins to

* To whom correspondence should be addressed: (e-mail) andrea@gene.com.

† Department of Protein Engineering.

‡ Present address: Sunesis Pharmaceuticals, Inc., 3696 Haven Ave., Suite C, Redwood City CA, 94063.

§ Department of Bioorganic Chemistry.

(1) (a) Rizo, J.; Gierasch, L. M. *Annu. Rev. Biochem.* **1992**, *61*, 387−418. (b) Ball, J. B.; Alewood, P. F. *J. Mol. Recognit.* **1990**, *3*, 55−64. (c) Hanessian, S.; McNaughton-Smith, G.; Lombart, H.-G.; Lubell, W. D. *Tetrahedron* **1997**, *53*, 12789−12854.

(2) (a) Freidinger, R. M. *Curr. Opin. Chem. Biol.* **1999**, *3*, 395−406. (b) Ripka, A. S.; Rich, D. H. *Curr. Opin. Chem. Biol.* **1998**, *2*, 441−452. (c) Giannis, A.; Kolter, T. *Angew. Chem., Int. Ed. Engl.* **1993**, *32*, 1244−1267. (d) Nakanishi, H.; Kahn, M. In *Bioorganic Chemistry: Peptides and Proteins*; Hecht, S. M., Ed.; Oxford University Press: New York, 1998; pp 395−419.

(3) Souers, A. J.; Virgilio, A. A.; Rosenquist, A.; Fenuik, W.; Ellman, J. A. *J. Am. Chem. Soc.* **1999**, *121*, 1817−1825.

(4) Sidhu, S. S.; Lowman, H. B.; Cunningham, B. C.; Wells, J. A. *Methods Enzymol.* **2000**, *328*, 333−363.

(5) Dower, W. J. *Curr. Opin. Chem. Biol.* **1998**, *2*, 328−334.

(6) (a) Hoess, R. H. In *Combinatorial Chemistry and Molecular Diversity in Drug Discovery*; Gordon, E. M., Kerwin, J. F., Jr., Eds.; Wiley-Liss: New York, 1998; pp 389−399. (b) Nygren, P.-A.; Uhlen, M. *Curr. Opin. Struct. Biol.* **1997**, *7*, 463−469. (c) Smith, G. P.; Patel, S. U.; Windass, J. D.; Thornton, J. M.; Winter, G.; Griffiths, A. D. *J. Mol. Biol.* **1998**, *277*, 317−332. (d) Christmann, A.; Walter, K.; Wentzel, A.; Kratzner, R.; Kolmar, R. *Protein Eng.* **1999**, *12*, 797−806. (e) Colas, P.; Cohen, B.; Jesson, T.; Grishina, I.; McCoy, J.; Brent, R. *Nature* **1996**, *380*, 548−550. (f) Norman, T. C.; et al. *Science* **1999**, *285*, 591−595.

(7) Vita, C.; Vizzavona, J.; Drakopoulou, E.; Zinn-Justin, S.; Gilquin, B.; Menez, A. *Biopolymers* **1998**, *47*, 93−100.

(8) Vita, C.; et al. *Proc. Natl. Acad. Sci. U.S.A.* **1999**, *96*, 13091−13096.

10.1021/ja003369x CCC: $20.00
Published on Web 12/28/2000

small peptides or to non-peptide small molecules remains an extremely challenging problem.[9]

We have chosen instead to ask whether it is possible to design very small structured peptides in which a subset of the sequence, e.g., a β-turn, could be varied. A structurally biased peptide turn library might combine the small size and structural advantages of a peptidomimetic with the ease of biosynthetic library construction. Although several examples exist of stably structured all-natural peptides,[10] those features necessary for structural stability are very poorly understood. In particular, there has been little systematic or quantitative assessment of the effect of residue substitutions and noncovalent interactions on structure. Our inital goal was to develop a quantitative understanding of stability determinants in disulfide-cyclized β-hairpins.

Short peptides that form β-hairpins have been explored as model systems for β-sheet structure in natural and designed proteins.[11] NMR analysis of several model peptides has permitted qualitative assessment of factors contributing to hairpin stability and, in some cases, estimates of hairpin population.[11] However, most β-hairpins are only marginally stable, and there are no unambiguous methods for assigning populations of the relevant conformers. Recently, a backbone-cyclized peptide was proposed as a reference state for a fully folded β-hairpin, allowing the quantitation of folded populations in linear analogues and the calculation of relative turn energies.[12]

Alternatively, thiol−disulfide equilibria in cystine-cyclized peptides have long been used to measure the relative tendencies of different sequences to adopt β-turn conformations, both in isolation[13] and as part of a larger β-hairpin.[14] Although this method does not provide the detailed structural information that can be obtained by NMR, it requires no assumption of a two-state folding model; therefore, it is free of any bias that errors in the choice of fully folded and unfolded reference states might introduce. Avoiding such errors becomes particularly important as the stability of the structures increases (and the fraction of folded molecules deviates substantially from 0.5).

Here we describe a model system for measuring individual residue contributions to the stability of small, disulfide-constrained β-hairpin peptides and evaluate a series of 19 substitutions in a particular non-hydrogen-bonded (NHB) strand position. Surprisingly, we find that tryptophan is far superior to other amino acids at this guest site. We then reexamine a set of strand substitutions in peptides with different turn sequences, and in accord with previous work,[11,12,14] we find significant differences in hairpin stability associated with the different turns. Furthermore, we find that tryptophan is highly stabilizing in the strand site, regardless of the turn sequence. Finally, we observe linear free energy relationships suggesting that, in many cases, turn and strand contributions to hairpin stability are additive. On the basis of these observations, we propose our disulfide-cyclized β-hairpin peptide as a scaffold for β-turn display. The stem portion of our tryptophan hairpin peptide is sufficiently stable to structure a relatively unstable turn from CD4, suggesting that it may be generally useful for this purpose.

Experimental Section

Peptide Synthesis and Purification. Peptides were synthesized as C-terminal amides using standard Fmoc chemistry on a Pioneer synthesizer (PE Biosystems). Peptides were cleaved from resin by treatment with 5% triisopropylsilane in trifluoroacetic acid (TFA) for 1.5−4 h at room temperature. After removal of TFA by rotary evaporation, peptides were precipitated by addition of ethyl ether and then purified by reversed-phase HPLC (acetonitrile/H_2O/0.1% TFA). Peptide identity was confirmed by electrospray mass spectrometry. Peptides were converted to cyclic disulfides by dropwise addition of a saturated solution of I_2 in acetic acid and repurified by HPLC. Purified peptides eluted as single symmetric peaks on C18 analytical columns (0−40% acetonitrile in 40 min).

Measurement of Cysteine Effective Concentrations. Glutathione stock solutions were prepared by mixing 3 volumes of 0.2 M reduced glutathione (GSH) with 1 volume of 0.1 M oxidized glutatione (GSSG). Aliquots were stored at −80 °C and were stable for several months; use of a single batch within each peptide series eliminated any error in $\Delta\Delta G$ values that might arise from variability of total glutathione concentration. To allow comparison of C_{eff} values from different experimental series, the glutathione stock concentrations were standardized by amino acid analysis. Thiol−disulfide equilibria were established by mixing 50 μL of peptide stock (~3 mM in water) with 50 μL of glutathione stock, deoxygenating the acidic solution with vacuum/argon cycles from a Firestone valve, and then adding 300 μL of deoxygenated buffer by syringe (0.2 M Tris, pH 8.0; 1 mM EDTA; 67 mM Tris base to titrate glutathione), followed by further deoxygenation of the mixture. The final pH of all reaction mixtures was 8.10 ± 0.05. Solutions were stirred under argon and maintained at 20 °C in a water bath. After 1.5 h, successive aliquots (100 μL) were removed with a gastight syringe, immediately quenched by discharge into 400 μL of 31 mM HCl (final pH ≤2) and analyzed by HPLC with a minimum of delay. Effective concentration (C_{eff}) values were calculated from the molar ratios of the reduced and oxidized forms of peptide and glutathione (peak area ratios corrected for absorbance differences measured by HPLC at 230 nm), assuming 0.025 M total glutathione monomer (i.e., neglecting the minor amount (<1%) of glutathione present in mixed disulfides with peptide):

$$C_{eff} = ([\text{peptide}_{ox}]/[\text{peptide}_{red}])([\text{GSH}]^2/[\text{GSSG}])$$

$$[\text{GSH}] + 2[\text{GSSG}] = 0.025\ \text{M}$$

$$[\text{GSSG}] = 0.025\ \text{M}/\{2 + 3.26(\text{GSH peak area}/\text{GSSG peak area})\}$$

$$[\text{peptide}_{ox}]/[\text{peptide}_{red}] = \text{peak area ratio}/\text{absorbance ratio}$$

Two or three samples from each reaction mixture were analyzed; there were no shifts in populations with time, and calculated C_{eff} values typically varied by less than 5% (equivalent to 30 cal mol^{-1} uncertainty in $\Delta\Delta G$). C_{eff} values (for selected peptides) were independent of peptide concentration.

NMR Spectroscopy and Structure Calculations. NMR samples contained 5−10 mM peptide in 92% H_2O/8% D_2O, pH 5.1, with 0.1 mM 1,4-dioxane as chemical shift reference. All spectra were acquired on a Bruker DRX-500 or a Varian Unity-400 spectrometer at 7, 17, or 27 °C. 2QF-COSY, TOCSY, and ROESY spectra were acquired as described[15] using gradient coherence selection[16] or excitation sculpting[17]

(9) Cochran, A. G. *Chem. Biol.* **2000**, *7*, R85−R94.

(10) For recent examples discovered from phage-displayed peptide libraries, see: (a) Lowman, H. B.; Chen, Y. M.; Skelton, N. J.; Mortensen, D. L.; Tomlinson, E. E.; Sadick, M. D.; Robinson, I. C. A. F.; Clark, R. G. *Biochemistry* **1998**, *37*, 8870−8878. (b) Dennis, M. S.; Eigenbrot, C.; Skelton, N. J.; Ultsch, M. H.; Santell, L.; Dwyer, M. A.; O'Connell, M. P.; Lazarus, R. A. *Nature* **2000**, *404*, 465−470.

(11) (a) Gellman, S. H. *Curr. Opin. Chem. Biol.* **1998**, *2*, 717−725. (b) Ramirez-Alvarado, M.; Kortemme, T.; Blanco, F. J.; Serrano, L. *Bioorg. Med. Chem.* **1999**, *7*, 93−103.

(12) Syud, F. A.; Espinosa, J. F.; Gellman, S. H. *J. Am. Chem. Soc.* **1999**, *121*, 11577−11578.

(13) (a) Milburn, P. J.; Konishi, Y.; Meinwald, Y. C.; Scheraga, H. A. *J. Am. Chem. Soc.* **1987**, *109*, 4486-4496. (b) Milburn, P. J.; Meinwald, Y. C.; Takahashi, S.; Ooi, T.; Scheraga, H. A. *Int. J. Pept. Protein Res.* **1988**, *31*, 311−321. (c) Falcomer, C. M.; Meinwald, Y. C.; Choudhary, I.; Talluri, S.; Milburn, P. J.; Clardy, J.; Scheraga, H. A. *J. Am. Chem. Soc.* **1992**, *114*, 4, 4036−4042.

(14) Stroup, A. N.; Gierasch, L. M. *Biochemistry* **1990**, *29*, 9765−9771.

(15) Cavanagh, J.; Fairbrother, W. J.; Palmer, A. G.; Skelton, N. J. *Protein NMR Spectroscopy, Principles and Practices*; Academic Press: San Diego, 1995.

(16) van Zijl, P. C. M.; O'Neil Johnson, M.; Mori, S.; Hurd, R. E. *J. Magn. Reson.* **1995**, *113A*, 265−270.

(17) Hwang, T.-L.; Shaka, A. J. *J. Magn. Reson.* **1995**, *112A*, 275−279.

Chart 1. Peptide Turn Variants

1	Ac-CT**X**E**GN**KLTC-NH_2	II′	
2	Ac-CT**X**E**NG**KLTC-NH_2	I′	**X** = W, Y, L, V, T, D
3	Ac-CT**X**E**pN**KLTC-NH_2	II′	p ≡ D-pro
4	Ac-CT**X**E**pG**KLTC-NH_2	II′	

for water suppression. Proton resonances were assigned by standard methods.[18] $^3J_{H^N-H^\alpha}$ were obtained by fitting Lorentzian lines to the antiphase doublets of H^N-H^α peaks in 2QF−COSY spectra processed to high digital resolution in F_2. ROESY and COSY-35 spectra were also acquired on samples in 100% D_2O. $^3J_{H^N-H^\beta}$ were extracted from the COSY-35 spectra. Distance and dihedral angle restraints were generated as described.[19] No explicit hydrogen bond restraints were included. A total of 100 initial structures were calculated using the hybrid distance geometry/simulated annealing program DGII;[20] 80 of these were further refined by restrained molecular dynamics using the AMBER all-atom force field implemented in DISCOVER as described previously.[19] A total of 20 conformations of lowest restraint violation energy were chosen to represent the solution conformation of each peptide. A geometric mean was calculated after global optimization of the pairwise RMSDs between backbone atoms, and a minimized mean structure was generated from this by restrained energy refinement with DISCOVER using the AMBER force field. In all cases, the resulting ensembles and minimized means had no distance restraint violations of >0.1 Å or dihedral angle restraint violations of >3°. All residues had backbone conformations in "preferred" or "allowed" regions of ϕ,ψ space.[21] Resonance assignments, coupling constants, and structural statistics for tryptophan peptides **1**-**3** (Chart 1) are listed in the Supporting Information.

NMR Analysis of CD4 Peptides. NMR samples of CD4 peptides contained ∼2 mM peptide in 92% H_2O/8% D_2O, pH 3.5 with 50 μM 3-(trimethylsilyl)-1-propane-*1,1,2,2,3,3-d*$_6$-sulfonic acid (DSS) as a chemical shift reference. Spectra were acquired at 15 °C and analyzed as described above. Resonance assignments, coupling constants, and statistics for the structure of cd2 are included in the Supporting Information.

Analysis of Side-Chain Rotamers. Observation of both $^3J_{H^\alpha-H^{\beta1}}$ and $^3J_{H^\alpha-H^{\beta2}}$ in the range of 6−9 Hz indicates that a side chain does not occupy a single classical rotamer ($\chi_1 = -60°$, +60°, or 180°) and most likely samples all three staggered rotamer wells. This is the situation for Trp3 and Leu8 of bhpW (peptide **1**) and Gln4, Phe7, and Leu8 of cd2. ROE peaks observed to these side chains represent a time-average over the range of χ_1 values sampled. Not all of these conformations will give rise to readily observable ROE peaks; hence, the structure calculation process will be biased toward those rotamers for which restraints could be obtained. For example, ROEs from Phe7 of cd2 are observed to protons in the opposite strand, thereby forcing Phe7 to lie in the +60° rotamer well. Given the large number of backbone−backbone distance and ϕ dihedral angle restraints, the structures calculated for bhpW and cd2 do accurately represent the solution conformation of these peptides, except in the overdetermination of some side-chain orientations.

Competition Binding Assays. To test whether peptides could bind to gp120, we used a BIAcore competition assay. Soluble CD4 (domains 1−4) was immobilized on a CM5 chip (Pharmacia Biosensor) using standard amine coupling procedures, and then $gp120_{MN}$ was injected alone or after preincubation with peptide. Buffer and regeneration conditions were as described.[22] Bound gp120 was determined from the increase in resonance units remaining after sample injection. We observed no significant decrease (<2%) in bound gp120 in the presence of 100 μM native CD4 peptide (cd1a) or the structured peptide cd2a; at higher peptide concentrations, adsorption of the peptides to the chip prevented accurate determination of bound gp120. As a control, we tested an inhibitory peptide (12p1) discovered by phage display.[23] This peptide almost completely blocked gp120 binding in our assay (87% inhibition at 100 μM).

To test peptides at concentrations higher than 100 μM, we used a competition ELISA similar to those previously described.[8,23] Peptides cd1a and cd2a failed to inhibit the binding of $gp120_{LAI}$ or $gp120_{IIIB}$ to immobilized CD4 at peptide concentrations of up to 1 mM. Again, the control peptide 12p1[23] was a potent inhibitor (IC_{50} ∼1 μM).

Results

Design of a Structured β-Turn Scaffold. We chose to investigate disulfide-constrained β-hairpins of the form CX_8C as scaffolds for β-turn display. The use of optimal turn sequences has been critical in reported β-hairpin designs.[11] However, for our purpose, it is essential to design a structure compatible with many turn sequences. That is, residues other than those in the turn must significantly bias the peptide toward hairpin structure. Disulfide cyclization is helpful, although not sufficient to structure many peptides. Our initial objective was to determine whether the disulfide bond could be used not only as a covalent constraint but also to nucleate a more extended interaction of the β-strands.

In our survey of β-sheets from a set of 928 nonredundant protein structures,[24] the mean $C^\beta-C^\beta$ distances between hydrogen-bonded and non-hydrogen-bonded pairs of residues in adjacent strands were 4.82 ± 0.58 and 5.37 ± 0.56 Å, respectively, while the average $C^\beta-C^\beta$ distance in disulfide-bonded cysteines was 3.84 Å (R.S.M., unpublished results). Therefore, the C^β atoms of opposing residues on antiparallel strands are normally too far apart for disulfide bond formation. Nonetheless, disulfide cross-links are sometimes found between cysteines in the non-hydrogen-bonding register in β-sheets.[25,26] We found 23 disulfide-bonded cysteine pairs joining adjacent antiparallel strands. In 14 of 23 cases, the disulfide packs tightly against the hydrophobic side chain two residues before one (or both) of the cysteines (Figure 1A). [In five additional cases this hydrophobic site was occupied by a polar or charged residue with β- and γ-methylenes (E, Q, or R)]. In particular, the side chains of either leucine or an aromatic amino acid provided good shape complementarity to this characteristic disulfide conformation. Accordingly, we chose leucine as residue 8 in our model peptide **1** (Figure 1B), included threonines at positions 2 and 9 to promote an extended backbone conformation, and chose the turn sequence EGNK as a representative, but not overly strong, type II′ β-turn. To determine the best cross-strand pairing with leucine, position 3 was varied.

The presence of a disulfide provides a sensitive, quantitative probe for hairpin structure. The equilibrium between peptide dithiol and cyclic disulfide can be measured relative to the reference thiol glutathione and expressed as an effective concentration (C_{eff}) for the cysteine pair:[27]

$$C_{eff} = ([GSH]^2 \cdot [peptide_{ox}])/([GSSG] \cdot [peptide_{red}]) \quad (1)$$

Larger values of C_{eff} indicate an increased proximity, on average,

(18) Wüthrich, K. *NMR of Proteins and Nucleic Acids*; John Wiley and Sons: New York, 1986.
(19) Skelton, N. J.; Garcia, K. C.; Goeddel, D. V.; Quan, C.; Burnier, J. P. *Biochemistry* **1994**, *33*, 13581−13592.
(20) Havel, T. F. *Prog. Biophys. Mol. Biol.* **1991**, *56*, 43−78.
(21) Laskowski, R. A.; MacArthur, M. W.; Moss, D. S.; Thornton, J. M. *J. Appl. Crystallogr.* **1993**, *26*, 283−291.
(22) Wu, H.; Myszka, D. G.; Tendian, S. W.; Brouillette, C. G.; Sweet, R. W.; Chaiken, I. M.; Hendrickson, W. A. *Proc. Natl. Acad. Sci. U.S.A.* **1996**, *93*, 15030−15035.
(23) Ferrer, M.; Harrison, S. C. *J. Virol.* **1999**, *73*, 5795−5802.
(24) Hobohm, U.; Sander, C. *Protein Sci.* **1994**, *3*, 522−524.
(25) Gunasekaran, K.; Ramakrishnan, C.; Balaram, P. *Protein Eng.* **1997**, *10*, 1131−1141.
(26) Hutchinson, E. G.; Sessions, R. B.; Thornton, J. M.; Woolfson, D. N. *Protein Sci.* **1998**, *7*, 2287−2300.
(27) Lin, T.-Y.; Kim, P. S. *Biochemistry* **1989**, *28*, 5282−5287.

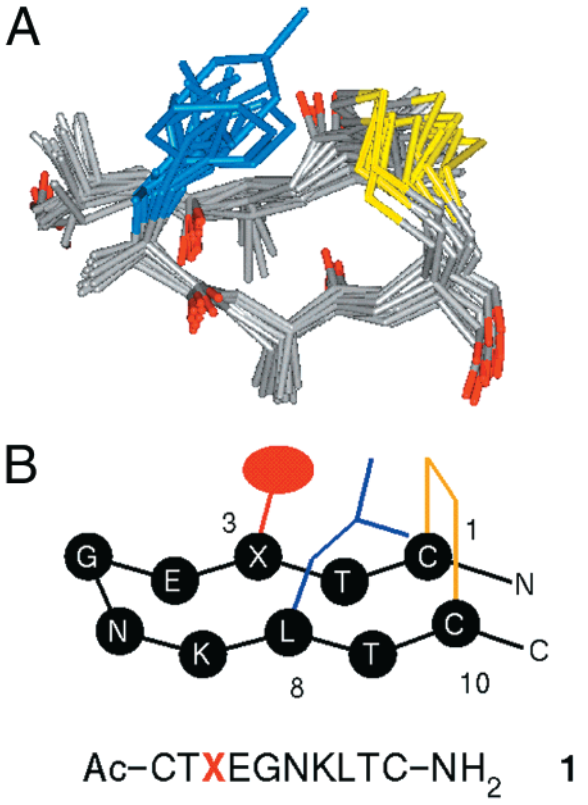

Figure 1. Design of the hairpin scaffold. (A) Superimposed structures of antiparallel β-strands illustrating the packing between disulfides (in yellow) and side chains of the closest non-hydrogen-bonded residues (blue). PDB codes (with the residue number of the blue side chain in parentheses) are as follows: 1A7S (179); 1AXI (B120 and B46); 1BU8 (A2); 1EBP (A26 and A36); 1GC1 (G294); 1GNH (A95); 1NCO (A45); 1P04 (A157); 1PRT (F25); and 2QWC (445). Figures 1A, 3, 6, and 7B were made using the program INSIGHT97.0 (Molecular Simulations, Inc.). (B) Schematic representation of the model hairpin peptide **1** with the side chains of the non-hydrogen-bonded residues 1, 3, 8, and 10 shown; the sequence is shown below. X represents the varied residue.

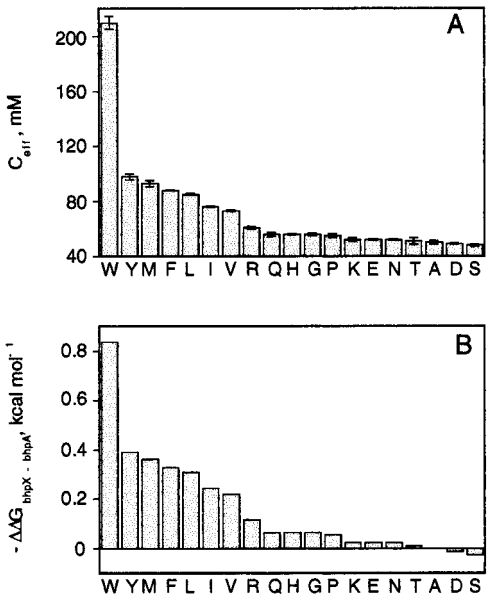

Figure 2. Relative hairpin stability for substitutions X in peptide **1** (Figure 1B). (A) Cysteine effective concentrations (C_{eff}) relative to glutathione. Error bars are for $\pm$ one standard deviation. (B) Equilibrium free energy differences relative to the alanine peptide ($T = 293$ K).

of the cysteine thiols, consistent with formation of the hairpin structure. C_{eff} ratios quantify the relative tendencies of different peptides to oxidize, and $\Delta\Delta G$ values calculated from these ratios have been interpreted as differences in structural stability.[13,14,27]

Peptide C_{eff} values varied significantly for different residues at position 3 (Figure 2A). Strikingly, tryptophan at position 3 strongly shifted the peptide equilibrium toward the oxidized form: this behavior was not caused by peptide aggregation or a failure to reach equilibrium.[28] Scaling of the C_{eff} values to that of the alanine analogue ($-RT \ln\{C_{eff,\,X}/C_{eff,\,Ala}\}$) yields free energy differences spanning > 0.8 kcal/mol (Figure 2B). These data do not, however, distinguish between effects on the folded and unfolded states of the peptide.[27] For example, a given substitution might promote favorable side-chain packing in the oxidized peptide or simply bias toward an extended backbone conformation in the reduced peptide.

Structural Validation of Effective Concentration Measurements. To assess whether the peptides were indeed forming β-hairpins, several of them were evaluated by ^{1}H NMR spectroscopy (Table 1). The tryptophan variant of peptide **1** (bhpW) exhibited all the hallmarks of a highly populated β-hairpin in terms of intense sequential $H^\alpha - H^N$ NOEs, numerous backbone cross-strand NOEs, and large backbone scalar coupling constants ($^3J_{H^N-H^\alpha} > 8.0$ Hz) for strand residues.[18] The H^α chemical shifts for Cys1 and Cys10 were downfield relative to values observed in unstructured peptides, indicating that the antiparallel strands encompass these terminal residues.[29] The other peptides studied were judged to have a lower population of hairpin structure (see Table 1). Importantly, the NMR data correlate well with C_{eff} (Table 1); thus, the disulfide exchange assay provides a useful quantitation of the degree of hairpin structure in the oxidized peptides.

Table 1. Comparison of Cysteine Effective Concentrations (C_{eff}) and ^{1}H NMR Data for Selected Variants of Hairpin Peptide **1**[a]

residue 3 (X, Figure 1b)	C_{eff}, mM	no. of $^3J_{H^N-H^\alpha} > 8$ Hz	δ Cys1 H^α, ppm	δ Cys10 H^α, ppm
Trp bhpW	210 ± 4	7	5.20	5.00
Tyr	98 ± 2	7	5.07	4.91
Phe	88 ± 0	5	5.07	4.92
Leu	85 ± 1	6	5.04	4.89
Val	73 ± 0	4	4.97	4.85
Lys	52 ± 2	3	4.92	4.82
Asn	51 ± 1	3	4.84	4.76
random coil		0	4.71	4.71

[a] The maximum number of strand residues with $^3J_{H^N-H^\alpha} > 8$ is 8; for the tryptophan peptide (bhpW), the Leu8 coupling constant is 7.9 Hz. Random coil coupling constants are taken from Smith et al.[31] Random coil H^α chemical shifts are taken from Wishart et al.[29]

Structures calculated for bhpW reveal a well-formed antiparallel hairpin with a type II′ turn (Gly5-Asn6) and hydrophobic contacts between the side chains of Cys1, Trp3, Leu8, and Cys10 (Figure 3, Supporting Information). Thermodynamic analysis of bhpW stability was complicated by the failure of the oxidized peptide to unfold fully, either at high temperature or in the presence of chemical denaturants. Nevertheless, we estimate the hairpin conformation to be highly populated, most likely >80%, at 15 °C.[30] Because of its structural stability, we have chosen bhpW for investigation as a turn display scaffold.

(28) C_{eff} for tryptophan peptide **1** was independent of concentration (2-fold and 4-fold dilution of original stock). At the 10−20-fold higher concentrations used in the NMR studies, no line broadening was observed for either the reduced or the oxidized peptide. In addition, approaching equilibrium from reduced instead of oxidized peptide did not change C_{eff} significantly ($\Delta\Delta G < 50$ cal/mol).

(29) Wishart, D. S.; Sykes, B. D.; Richards, F. M. *Biochemistry* **1992**, *31*, 1647−1651.

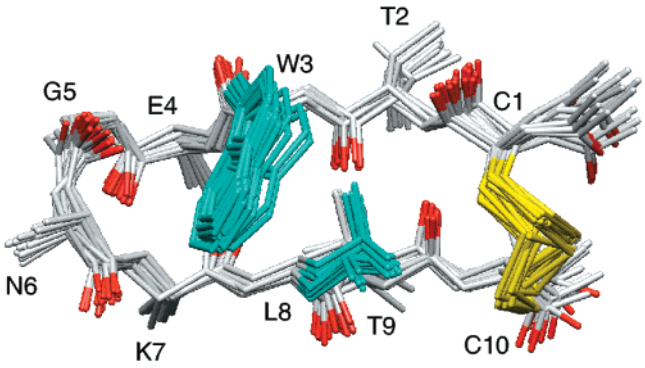

Figure 3. Structures (20 models) of bhpW (Trp analogue of peptide **1**) showing the packing of Cys1, Cys10, and Trp3 onto Leu8. For clarity, the side chains of Glu4, Asn6, and Lys7 are truncated at C^{β}; backbone carbonyl oxygens are red, Trp3 and Leu8 side chains are cyan, and cysteine side chains are yellow. The mean backbone RMSD for the 20 models, with respect to the mean coordinates of residues 1−10, is 0.37 Å. The measured $^{3}J_{H^{\alpha}-H^{\beta}}$ coupling constants for Trp3 and Leu8 indicate the population of more than one side-chain rotamer (see Methods).

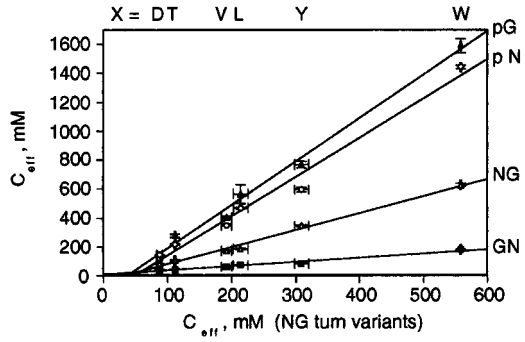

Figure 4. Effective concentration (C_{eff}) values for substitutions X in peptides with different turns (Chart 1). The strand substitutions X are shown at the top of the graph, and the central residues of the turns are indicated to the right. Values are averages for two or more measurements from one or more samples. Error bars indicate ± 1 standard deviation. C_{eff} values for the Asn−Gly (NG) series were determined in two sets of experiments (see Table 2).

Effect of Different Turns on Hairpin Stability. The guest site (position 3, X) is quite close in space to the type II′ turn (Gly−Asn, Figure 3). We therefore wondered whether hairpins with different turn sequences and geometries would have different residue preferences at the NHB guest site. To investigate this, we replaced the central Gly−Asn sequence in our hairpin **1** (Chart 1) with the type I′ turn Asn−Gly (peptide **2**) and the type II′ turns D-Pro−Asn and D-Pro−Gly (peptides **3** and **4**). Substitutions at position 3 (X) were chosen to span the range of hairpin stabilities we observed in the Gly−Asn series (Figure 2). The values we obtain for the different turns are compared in Figure 4.

Table 2. Turn Energies Relative to Asn−Gly in Peptides **1**−**4**

turn sequence	C_{eff} correlation slope	C_{eff} correlation R^2	$\Delta\Delta G$, kcal mol^{-1} [a]
Asn−-Gly repeat[b]	1.19	0.99	−0.10
Gly−Asn	0.29	0.97	0.72
D-Pro−Asn	2.72	0.98	−0.58
D-Pro−Gly[c]	3.01	0.99	−0.64

[a] $\Delta\Delta G = -RT \ln(\text{slope})$, $T = 293$ K. Slopes are from the plot in Figure 4. [b] A second, independent set of measurements (with different reagents) was made for the Asn−Gly peptides in order to assess the reliability of the assay. $\Delta\Delta G$ for the two data sets (∼0.1 kcal mol^{-1}) may be taken as an estimate of the error in the turn energies reported here. [c] $\Delta\Delta G$ may be compared to the value of -0.52 ± 0.11 kcal mol^{-1} (277 K) recently reported by Syud et al.[12]

In all cases, tryptophan at position 3 yields the largest C_{eff} value for a given turn, demonstrating that its stabilizing influence is general. The large changes in C_{eff} for the different cross-strand interactions (horizontal axis) and turn sequences (vertical axis) show that both can contribute significantly to stability in these cyclic hairpin peptides (Figure 4). Finally, there are striking linear correlations between data sets, indicating that substitutions at strand position 3 and the turn replacements make independent contributions to stability of the cyclic hairpin. These data suggest that the hairpin fold may be quite modular, which would significantly simplify hairpin design.

Relative turn energies can be calculated by comparing C_{eff} for the appropriate pairs of peptides.[13,14] However, the correlations in Figure 4 allow the calculation of relative turn energies from the slopes, which should be less sensitive to experimental error.[32] These values are listed in Table 2. Compared to Asn−Gly (type I′), Gly−Asn (type II′) is less stabilizing, while the D-Pro-containing turns (also type II′) enhance hairpin stability. In the one case where a comparison may be made, Asn−Gly vs D-Pro−Gly, the $\Delta\Delta G$ value obtained here agrees reasonably well with that obtained by NMR.[12,33] This suggests that the reference states assigned by Syud et al.[12] and their assumption of two-state folding are appropriate for their model system; however, defining such reference states is not always feasible.

Alternatively, substitution energies for strand position 3 may be obtained by plotting the same data, grouped instead by the substituted residue X (not shown). The correlations are again excellent, and the slopes yield the free energy changes (Table 3). The range of energies is larger than we observed for peptide **1** (1.42 vs 0.85 kcal mol^{-1}). Much of the difference is traced to those substitutions at the bottom of the stability scale (particularly Asp). The less stable of the Gly−Asn turn peptides are not detectably structured (Table 1), and C_{eff} assays do not register any difference between them (Figure 2A). Thus, the data obtained in peptides with the stronger turn sequences provide a more complete view of the strand substitution energies, while confirming the general superiority of tryptophan in the guest position.

Finally, the energetic relationship between position 3 strand substitutions and the various turns is emphasized in Figure 5.

(30) We attempted to measure the stability of bhpW by a variety of methods (data not shown). C_{eff} values for folded proteins are expected to be sensitive to added urea,[27] but even at 7.5 M urea, bhpW retains structure ($\Delta\Delta G_{0\ M-7.5\ M} = 0.2$ kcal mol^{-1}). Circular dichroism (CD) signal (215 nm) is nonlinear with temperature, but there is insufficient baseline (folded or unfolded) to fit the data to a two−state model. At temperatures between 15 and 55 °C, 7 of 8 $^{3}J_{H^{N}-H^{\alpha}}$ remained >8 Hz (see Table 1), suggesting little change in structure. Finally, at low temperature, the CD spectrum and H^{α} chemical shifts are relatively insensitive to added methanol (used to drive hydrogen bonding in hairpin model systems: Maynard, A. J.; Sharman, G. J.; Searle, M. S. *J. Am. Chem. Soc.* **1998**, *120*, 1996−2007), suggesting that in water the fraction of structured molecules is high.

(31) Smith, L. J.; Bolin, K. A.; Schwalbe, H.; MacArthur, M. W.; Thornton, J. M.; Dobson, C. M. *J. Mol. Biol.* **1996**, *225*, 494−506.

(32) We did find that the correlation between the Asn−Gly and D-Pro−Asn data was not as good with an expanded set of substitutions X ($R^2 = 0.88$ for 14 points). Nevertheless, the deviations are small compared to the total range of C_{eff} in the two series and occur mainly near the bottom of the stability range. Inclusion of these data does not significantly change the slope of the plot or the relative turn energy given in Table 2.

(33) However, the energy reported by Syud et al.[12] was measured in the turn background VXXK, while our turn sequence is EXXK. Although there appear to be small differences in the residue distributions at position *i* (E4 in our peptides) of type I′ and type II′ turns in proteins, these differences are not statistically significant (Hutchinson, E. G.; Thornton, J. M. *Protein Sci.* **1994**, *3*, 2207−2216). We have not determined whether replacing Glu with Val changes the relative stability of the Asn−Gly and D-Pro−Gly turns.

Table 3. Relative Energetic Contributions from Strand Residue X

residue X	slope[a]	$\Delta\Delta G$, kcal mol^{-1} [b]	$\Delta\Delta G$, GN turn[c]
Trp	2.92	−0.62	−0.53
Tyr	1.27	−0.14	−0.08
Leu		0	0
Val	0.66	0.24	0.09
Thr	0.45	0.46	0.30
Asp	0.25	0.80	0.32

[a] C_{eff} values were plotted against those of leucine peptides **1**−**4**. [b] $\Delta\Delta G = -RT \ln(\text{slope})$, $T = 293$ K. [c] $\Delta\Delta G$ for the Gly−Asn turn series ($\Delta\Delta G = -RT \ln\{C_{eff,\,X}/C_{eff,\,Leu}\}$).

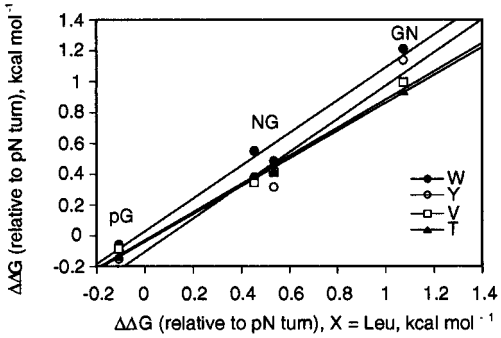

Figure 5. Comparison of relative turn energies (vs D-Pro−Asn, series **3**) for various strand substitutions X. $\Delta\Delta G$ for X = Trp, Tyr, Val, and Thr are plotted against $\Delta\Delta G$ for X = Leu.

Comparing relative turn free energies for individual strand substitutions reveals correlations with slopes very close to 1, demonstrating that, for these peptides, the turns and adjacent NHB cross-strand pairs are energetically independent. Because these components contribute independently to hairpin stability, the general utility of the hairpin stem in structuring turn sequences should be limited only by the limitations in attainable cross-strand interaction energies.

To assess how the turn types affect hairpin structure, the tryptophan analogues of **2** and **3** (Chart 1) were characterized by NMR spectroscopy, and structures were calculated (see Supporting Information). The comparison of minimized mean structures in Figure 6 reveals that the backbone and side-chain conformations are very similar for the nonturn residues (RMSD ∼ 0.3 Å), regardless of the type of turn present. Thus, consistent with the observed linear free energy relationships (Figures 4 and 5), these three turns do not change the structure of the adjacent strands.

Interestingly, $^3J_{H^N-H^\alpha}$ for the non-hydrogen-bonded residues Trp3 and Leu8 are not as extreme as for other strand sites. Indeed, in peptides **1** and **2**, the value for Leu8 falls slightly below 8.0 Hz. A bending motion in the middle of the hairpin could give rise to such an effect. However, we see no other evidence for motion, such as temperature dependence of the chemical shifts or line widths (not shown). A $^3J_{H^N-H^\alpha}$ value of 7.5 Hz is consistent with a phi angle of approximately −80° (compared to typical values of −100° to −140° in β-sheets). However, in two-stranded antiparallel structures, a less negative ϕ angle is often observed for the non-hydrogen-bonded residues, giving rise to a coiling of the β-strands.[34] In the cocrystal structure of the disulfide-cyclized β-hairpin peptide EMP-1 and erythropoietin receptor,[35] peptide residues Phe8 and Trp13 (analogous to Trp3 and Leu8 of bhpW) have similar ϕ angles

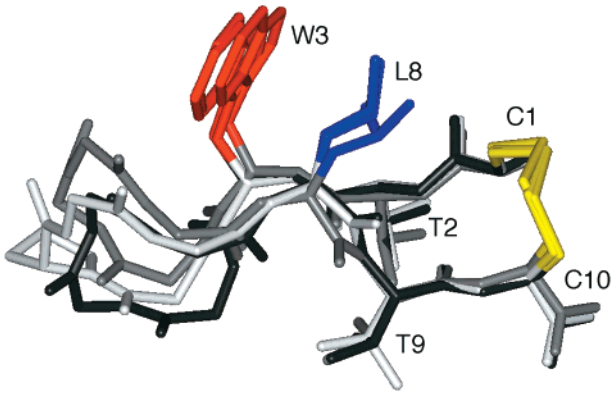

Figure 6. Minimized mean structures of the tryptophan analogues of peptides **1** (gray, bhpW, GN turn), **2** (black, NG turn) and **3** (white, pN turn) overlaid on the backbone atoms of residues 1−3 and 8−10 (RMSD of 0.36 and 0.30 Å for **1** with respect to **2** and **3**, respectively). Side chains for the hydrophobic NHB strand residues are shown colored as in Figure 1B. For clarity, nonproline side chain atoms of the four turn residues are not shown.

(−44° to −75°). Thus, the coupling constants observed here probably reflect twist in the hairpin scaffold rather than dynamic behavior.

Use of the Tryptophan Scaffold To Present a β-Turn from CD4. The β-turns in our model peptides **2**−**4** are exceptionally strong and do not, therefore, reflect the majority of turns found in proteins. Accordingly, we investigated whether our tryptophan peptide scaffold was sufficiently stable to structure a weaker turn sequence taken from a protein loop. From the linear free energy relationships described above, we expect the folded conformation of a transferred turn to be determined by its sequence,[36] while the fraction of molecules adopting this conformation will be determined by the relative energies of the turn and of the cross-strand interactions present in the tryptophan scaffold.

A recent crystal structure of HIV gp120 bound to a neutralizing antibody and to the human T cell-surface protein CD4 revealed details of the contact surfaces.[37] As had been anticipated from numerous mutagenesis studies, the CD4 region most important for gp120 binding is the C′−C″ hairpin loop (residues 37−46), with the critical Phe43 side chain extending from the protein surface. In fact, CD4 residues 40−48 contribute 63% of the surface area buried in the interface, with 23% of the total contributed by Phe43.[37] Unexpectedly, there is a large cavity in gp120, behind the Phe43 binding site, that is lined with hydrophobic residues. It seemed possible that a structured peptide based on the C′−C″ turn might bind to gp120 and, if so, might be a starting point for designing ligands that extend into the cavity seen in the crystal structure.

We synthesized a disulfide-constrained peptide based on the native sequence of the CD4 hairpin (residues 38−45, cd1 in Table 4) and found it to be essentially unstructured in solution (Table 4, Figure 7A). We then made the substitutions Gly2Thr and Asn3Trp, to match the corresponding residues in bhpW (cd2, Table 4); residues Leu8 and Thr9 are already present in the native CD4 sequence. Trp3 and Thr2 should be positioned away from the gp120 contact surface and, therefore, should not interfere sterically with binding. Peptide cd2 is well-ordered,

(34) (a) Chothia, C. *J. Mol. Biol.* **1983**, *163*, 107−117. (b) Yang, A.-S.; Honig, B. *J. Mol. Biol.* **1995**, *252*, 366−376.

(35) Livnah, O.; Stura, E. A.; Johnson, D. L.; Middleton, S. A.; Mulcahy, L. S.; Wrighton, N. C.; Dower, W. J.; Jolliffe, L. K.; Wilson, I. A. *Science* **1996**, *273*, 464−471.

(36) For an example of such a structural transfer in a protein, see: Hynes, T. R.; Kautz, R. A.; Goodman, M. A.; Gill, J. F.; Fox, R. O. *Nature* **1989**, *339*, 73−76.

(37) Kwong, P. D.; Wyatt, R.; Robinson, J.; Sweet, R. W.; Sodroski, J.; Hendrickson, W. A. *Nature* **1998**, *393*, 648−659.

Table 4. Comparison of Tryptophan Peptide 1 (bhpW) and Peptides Based on the CD4 C′−C″ Loop[a]

peptide		C_{eff}, mM	$[\theta]_{215}$,[c] deg cm^2 dmol^{-1}	no. of $^3J_{H^N-H^\alpha} > 8$ Hz[d]	δ (Cys_N H^α),[e] ppm	δ (Cys_C H^α),[f] ppm
Ac−C*TW*EGNKLTC−NH_2	bhpW	210 ± 4	−19800	7	5.20	5.00
SC*TW*EGNKLTCK−NH_2		273 ± 2	−17400	7	5.47	5.24
Ac−C*GN*QGSFLTC−NH_2	cd1	nd	nd	0	4.66	4.66
Ac−C*TW*QGSFLTC−NH_2	cd2	nd	−15800	6	5.08	4.93
SC*GN*QGSFLTCK−NH_2	cd1a	45 ± 4	−1500	0	4.80	4.72
SC*TN*QGSFLTCK−NH_2		nd[b]	−5000	2	4.96	4.79
SC*GW*QGSFLTCK−NH_2		48 ± 0	−6100	3	5.00	4.88
SC*TW*QGSFLTCK−NH_2	cd2a	120 ± 0	−14000	6	5.36	5.14

[a] Terminal serine and lysine residues were added to improve the solubility of some variants of the CD4 peptide, which are otherwise uncharged. A similar modification was made to bhpW as a control. Nonturn residues that differ between bhpW and the CD4 loop are in italics. nd, not determined. [b]Coelution of reduced and oxidized peptides prevented measurement of C_{eff} for the Thr2, Asn3 variant of the CD4 peptide. [c]Circular dichroism spectra were acquired at 10 °C with an Aviv Instruments, Inc. model 202 spectrophotometer; peptide concentrations were 20 μM in 20 mM potassium phosphate, pH 7.0. [d]The maximum number of strand residues with $^3J_{H^N-H^\alpha} > 8$ is 8. (Terminal lysines are not included in this number.) [e]Cys_N H^α: H^α chemical shift for the more N-terminal cysteine (Cys1 or Cys2) [f]Cys_C H^α: H^α chemical shift for the more C-terminal cysteine (Cys10 or Cys11).

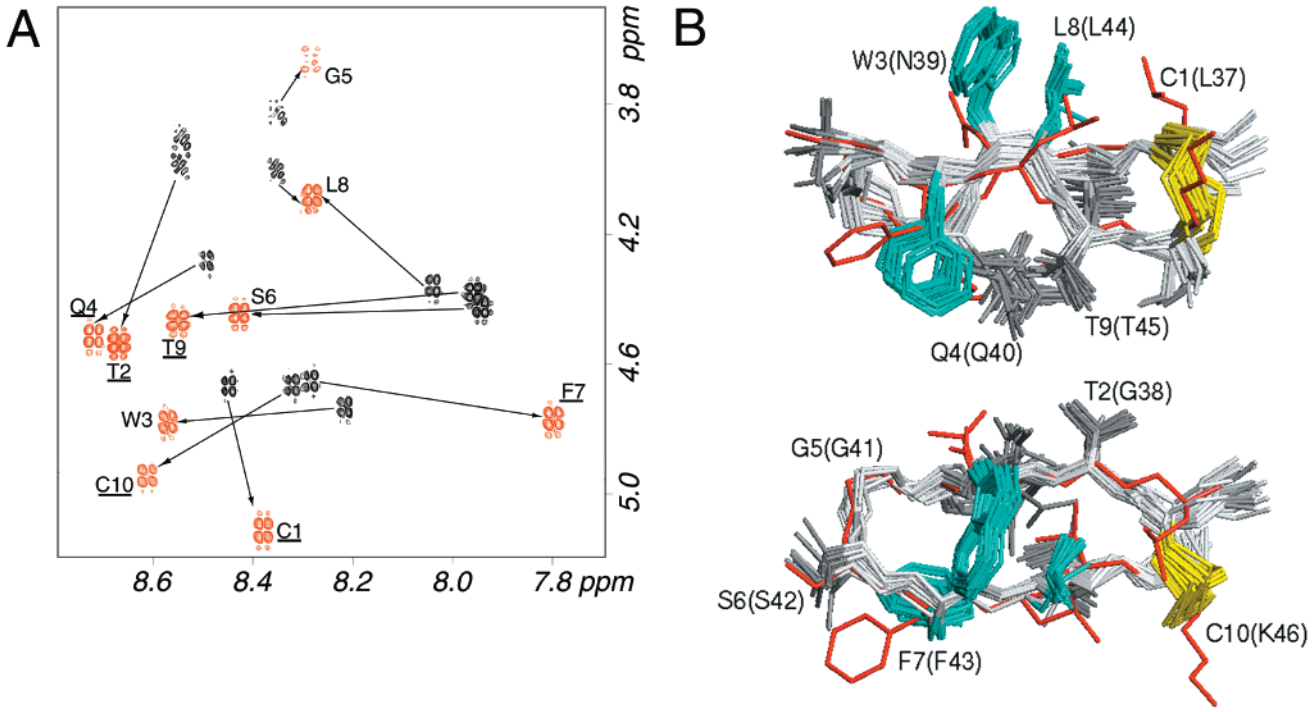

Figure 7. NMR analysis of CD4 peptides. (A) Overlay of the fingerprint region of the COSY spectra for cd1 (black) and cd2 (red). Peak assignments for cd2 are shown; arrows indicate the location of the corresponding cross-peak in cd1. Those cd2 residues with $^3J_{H^N-H^\alpha} > 8.3$ Hz are underlined; all cd1 residues have backbone coupling constants between 5.9 and 7.7 Hz. (B) NMR structure ensemble for cd2 (20 models; two orthogonal views) shown superimposed on CD4 residues 37−46 (red) from the crystal structure of gp120-bound CD4 (PDB entry 1GC1[37]). The RMSD for the 20 models, with respect to the mean coordinates for the backbone atoms of residues 1−10, is 0.50 ± 0.09 Å; comparison of the mean coordinates of residues 1−10 with residues 37−46 of CD4 from the crystal structure yields an RMSD of 0.93 Å. Note that the $^3J_{H^\alpha-H^\beta}$ for Phe7 of cd2 indicate that this side chain is *not* fixed in the rotamer seen in the ensemble (see the Experimental Section); the Phe7 side chain adopts multiple conformations in solution, undoubtedly sampling that observed in the cocrystal structure.

adopting a hairpin structure with a type II′ turn (Table 4, Figure 7). From the C_{eff} ratios, the CD4 turn (QGSF) destabilizes the model hairpin (EGNK turn, peptide **1**) by 0.5 kcal/mol, and we found that both the Thr2 and Trp3 substitutions were necessary for stable hairpin structure (Table 4). Importantly, comparison of the peptide structure with that of CD4 indicates that the backbone conformations are essentially the same, within the uncertainties of the structure determinations [0.93 Å (residues 1−10) and 0.41 Å (turn residues 4−7) backbone RMSD; see Figure 7B]. This demonstrates that the peptide scaffold correctly presents the CD4 β-turn.

Although the C′−C″ turn region of CD4 is *necessary* for high-affinity binding to gp120, it is not known whether it might be *sufficient*. This information would be important in any effort to design small-molecule inhibitors based on the structure of CD4. Peptidomimetics have been designed previously to mimic this turn.[38,39] Although these compounds were reported to inhibit in cell-based assays, they were found later not to compete with CD4 for binding to gp120.[39] Unfortunately, structures of these mimetics were not determined, so it is difficult to interpret these data. Because our hairpin peptide does adopt the correct turn structure, we can now test whether this turn is sufficient for binding. We find that the CD4 peptide, despite its structural similarity to the protein, does not have significant affinity for gp120 ($IC_{50} \gg 1$ mM; see the Experimental Section).

In contrast, peptides displaying CD4 C′−C″ loop residues on charybdotoxin or scyllatoxin scaffolds (27−33 residues in

(38) Chen, S.; et al. *Proc. Natl. Acad. Sci. U.S.A.* **1992**, *89*, 5872−5876.
(39) Ramurthy, S.; Lee, M. S.; Nakanishi, H.; Shen, R.; Kahn, M. *Bioorg. Med. Chem.* **1994**, *2*, 1007−1013.

length) do compete with CD4 for binding to gp120 ($IC_{50} \approx 20-200\ \mu M$).[7,8] The NMR structure of the scyllatoxin mimetic (PDB code 1D5Q)[8] indicates that the conformation of the QGSF turn is indistinguishable from that observed in the CD4−gp120 complex and our peptide cd2.[40] However, the critical phenylalanine side chain (Phe23 of the scyllatoxin mimetic) is not fixed in the rotamer observed in the complex (and may largely populate the wrong rotamer),[8] demonstrating that rigid presentation of the phenyl ring is not required for binding to gp120. Notably, the scyllatoxin peptides incorporate CD4 binding determinants not present in our designed hairpin (G47 and P48, plus K35 and R59 surrogates). Therefore, the failure of our peptide to bind may be due to its inability to trigger gp120 conformational changes that normally accompany CD4 binding[41] or simply to insufficient contacts with gp120. In any case, it demonstrates that faithful presentation of the native β-turn does not guarantee affinity for gp120.

Discussion

Our results demonstrate that optimization of a single-strand position in a small disulfide-constrained hairpin is sufficient to convert a very poorly structured molecule to one that is highly structured ($-\Delta\Delta G > 0.8$ kcal mol^{-1}). The stem portion of the structured hairpin, −CTW- - - -LTC−, does not require an optimized turn sequence; thus, it is a suitable scaffold for display of β-turn libraries and for studying particular turns that might not otherwise be highly populated. Importantly, only natural amino acids are required, so turn libraries may be displayed on phage.

It is interesting to compare the strand substitution energies we report here with previous studies on β-sheet systems. Although the magnitude of the energy differences is similar, the rank order we obtain does not correlate with experimental β-propensity scales[42,43] or with observed residue pair frequencies in known β-sheets.[26,44] In particular, tryptophan is unexceptional in such scales. These differences stress that average trends in typical protein domains may not apply directly to small peptides in which most residues are highly solvent exposed, complicating the use of such information in de novo design. Furthermore, while the preferred residues are hydrophobic, $\Delta\Delta G$ does not correlate well with increasing nonpolar surface area of the side chains.

The relative importance of the turn sequence and good cross-strand pairing to hairpin structure has been addressed previously in many model studies.[11] However, these studies have yielded little quantitative data, precluding systematic evaluation of residue substitutions. Our data show that, for these simple cyclic peptides, substitutions in a strand site and in the turn have independent, additive effects on hairpin stability. This is perhaps unexpected, given their proximity in the structure (Figures 3 and 6). Nonetheless, it would appear that coupling between these turns and strands is negligible compared to the large influence each exerts alone.

It is interesting to consider what fraction of the 160 000 possible four-residue sequences might be expected to form β-turns when introduced into our peptide scaffold. Because of the additivity relationships we observe, the fraction of structured hairpins will depend on the distribution of turn energies for the various sequences. Presently, it is difficult to estimate what this distribution might be. (Certainly some particular sequences, e.g., VVVV,[13b] cannot adopt turn conformations compatible with our hairpin.) It has been shown that about three-quarters of inserted random sequences can replace a β-turn of protein G B1 domain without completely disrupting folding.[45] The stability of the wild-type protein G scaffold is −5.6 kcal mol^{-1}, and the fraction of viable turn sequences drops for lower stability mutants.[45] Unfortunately, since we cannot determine the absolute stability of the cyclized hairpins, we cannot compare the two scaffolds directly. It remains possible, therefore, that our peptide scaffold will structure a smaller number of turn sequences than does protein G. Nevertheless, very few of the turn sequences observed in proteins have ever been shown to adopt well-defined turn conformations in isolated peptides, and we have demonstrated a simple strategy to increase this number.

Finally, the hairpin stem is very small,[46] yet the combination of disulfide and cross-strand tertiary contact imparts a structural bias exceeding that of a disulfide alone, e.g., CX_4C.[47] We envision that hairpin libraries with randomized turn sequences (e.g., $XCTWX_4LTCX$, or further optimized variants[48]) might yield structured ligands whose binding determinants could be transferred readily to small synthetic turn mimetics[3] or even used directly to identify small-molecule leads for high-throughput affinity optimization.[49]

Acknowledgment. We thank Stephen Russell for assistance with peptide synthesis and purification and the Genentech Department of Protein Chemistry for amino acid analysis.

Supporting Information Available: Resonance assignments, coupling constants, and structural statistics for the peptides shown in Figures 3, 6, and 7. This material is available free of charge via the Internet at http://pubs.acs.org.

JA003369X

(40) All pairwise comparisons of backbone atoms from the four-residue turns yield RMSDs of ≤0.4 Å.

(41) Zhang, W.; Canziani, G.; Plugariu, C.; Wyatt, R.; Sodroski, J.; Sweet, R.; Kwong, P.; Hendrickson, W.; Chaiken, I. *Biochemistry* **1999**, *38*, 9405−9416.
(42) Muñoz, V.; Serrano, L. *Proteins* **1994**, *20*, 301−311.
(43) Minor, D. L., Jr.; Kim, P. S. *Nature* **1994**, *371*, 264−267.
(44) Wouters, M. A.; Curmi, P. M. G. *Proteins* **1995**, *22*, 119−131.
(45) Zhou, H. X.; Hoess, R. H.; DeGrado, W. F. *Nat. Struct. Biol.* **1996**, *3*, 446−451.
(46) For another example of a small structured peptide scaffold, see: McBride, J. D.; Freeman, N.; Domingo, G. J.; Leatherbarrow, R. J. *J. Mol. Biol.* **1996**, *259*, 819−827.
(47) For example, CD4 peptides of the form −CQGSFC− do not form the type II′ β-turn present in the protein and in peptides cd2 and cd2a [A.G.C.; M.A.S., unpublished results].
(48) Russell, S. J.; Cochran, A. G. *J. Am. Chem. Soc.* **2000**, *122*, 12600−12601.
(49) Rohrer, S. P.; et al. *Science* **1998**, *282*, 737−740.